

## EXPANDING THE APPLICATIONS OF COPPER-BASED ALLOYS BY THERMAL ARC SPRAYING

In this article, the case of depositing a Ni-based alloy layer by thermal arc spraying on a copper alloy substrate with cylindrical geometry over its entire surface is presented. After the coating was deposited, the layer was analyzed microstructurally both on the surface and in cross-section, and it was observed that it adhered very well to the substrate. In addition to the high adhesion to the substrate, a low porosity of the coating was observed, which ensures good compactness of the coating. Based on these results, further investigation of the Ni coating can be recommended to limit the toxicity caused by the oxidation of copper and copper alloy heating elements.

*Keyword:* Ni coating; copper-based heating elements; oxidation resistance

## 1. Introduction

Copper is the oldest material used by mankind, its first application being dated to about 10,000 years ago. Its use has evolved, being still one of the materials with extensive applications due to its excellent properties of thermal and electrical conductivity, corrosion resistance, good strength and fatigue resistance. Pure copper is widely used to make rods, wires and electrical contacts, and its alloys are used to produce radiators, heat exchangers, domestic and industrial heaters, panels for solar energy capture, pipes, valves, fittings for drinking water systems or for the circulation of other fluids [1,2]. However, there are also fewer desirable aspects of using copper, one of which is heating at high temperatures in the presence of air. This process involves a chemical oxidation reaction of copper, with the formation of  $\text{Cu}_2\text{O}$  and  $\text{CuO}$  oxides, the destructive process increasing exponentially with increasing temperature [3].

One of the technologies that has increasingly gained ground in Surface Engineering applications over the last 50 years due to its versatility is thermal spray deposition technology [4,5].

Thermal coating methods are techniques used to apply protective or functional coatings to various surfaces using heat. These coatings often provide thermal insulation, corrosion resistance, or other desirable properties. Some common thermal coating methods include [6]:

- Flame Spraying: In this method, combustible gas and oxygen are mixed and ignited, generating a high-velocity

flame. Powdered coating materials are introduced into the flame, melted, and propelled onto the substrate.

- Plasma Spraying: Plasma spraying involves using a plasma torch to ionize and heat a gas, typically argon, into a high-temperature plasma. The coating material, in the form of powder or wire, is injected into the plasma stream, melts, and is sprayed onto the substrate.
- Arc Spraying: In this method, an electric arc is created between two consumable wires (a coating material and a sacrificial wire) to produce molten droplets. These droplets are propelled onto the surface to form the coating.
- High-Velocity Oxygen Fuel (HVOF) Spraying: HVOF spraying utilizes a high-velocity oxygen-fuel flame to propel the coating material onto the substrate. The high velocity of the particles results in dense and well-adhered coatings.
- Wire Flame Spraying: In this process, a metallic wire is fed into a flame, melted, and sprayed onto the substrate. It is commonly used for applying corrosion-resistant coatings.
- Detonation Gun (D-Gun) Spraying: The D-Gun process involves a controlled detonation of oxygen and fuel mixtures to accelerate the coating material particles onto the substrate, achieving a dense and strong coating.
- Twin-Wire Arc Spraying: Similar to arc spraying, but uses two wires instead of one, resulting in higher deposition rates and improved coating properties.

<sup>1</sup> GHEORGHE ASACHI TECHNICAL UNIVERSITY OF IASI, DEPARTMENT OF MATERIALS SCIENCE AND ENGINEERING, BLVD. MANGERON, NO. 41, 700050, IASI, ROMANIA

\* Corresponding author: [daniela-lucia.chicet@academic.tuiasi.ro](mailto:daniela-lucia.chicet@academic.tuiasi.ro)



- Induction Heating: This method uses electromagnetic induction to heat a substrate, and then a coating material is applied, which melts and forms a bonded coating.
- Laser Cladding: A laser beam is used to melt a coating material (in the form of powder or wire) onto the substrate, resulting in a precise and well-adhered coating.
- Electron Beam Physical Vapor Deposition (EB-PVD): In this technique, an electron beam is used to evaporate a coating material, which then condenses onto the substrate, forming a thin and uniform coating.

Each of these thermal coating methods has its advantages and is suitable for specific applications based on factors like material type, substrate, desired coating properties, and cost-effectiveness.

The coatings thus obtained have been used for several decades to improve the characteristics of many functional surfaces, among which can be mentioned: abrasive wear [7], contact fatigue [8], corrosion resistance [9], resistance to sliding wear [10], high temperatures sollicitation [11], thermal insulation or biocompatibility [12].

The novelty of this study is the extending of the high-temperature copper applications without the risk of oxidation that leads to both material destruction and increased toxicity of the working environment as a result of the formation and release of copper oxides that can be achieved by coating the exposed surfaces with compact layers using the thermal spray method.

## 2. Experimental procedure

### 2.1. Materials and methods

In order to carry out our own research into the characteristics of thermal spray deposition, we began by determining the exact chemical composition and structure of the materials used. Determinations were carried out on the base material (substrate) and wires (filler material) prior to the sputtering process.

The substrate used was a commercial Cu alloy, grade CW024A (SR EN 105), rolled in the form of a round tube with an external diameter of Ø10 mm and a wall thickness of 1.5 mm. The results of the chemical analysis of the CW024A steel used are given in TABLE 1.

In the experimental research we used 1.6 mm diameter wire of material 75B produced by Tafa Group – USA. The chemical composition of the coating material is given in TABLE 2. The technical characteristics of the coating material guaranteed by the manufacturer are: porosity <15%, adhesion max. 68.55 N/mm<sup>2</sup>.

TABLE 1

Chemical composition of the CW024A material used

Material	Cu [%]	Si [%]	S [%]	P [%]	C [%]	Ag [%]
CW024A	99.8	—	—	0.022	—	balance

TABLE 2

Chemical composition of the input material

Material	C [%]	Mn [%]	Si [%]	Al [%]	Fe [%]	Ni [%]	Ti [%]
75B	—	—	—	rest	—	95-97	—

The coatings were deposited at a spray distance of 120 mm on cylindrical surfaces with a roughness of 14.3 µm and on a set of lamellar specimens required for adhesion testing. The entraining and atomizing gas used was compressed air produced by a Kaeser SM15 compressor.

TABLE 3 shows the technological process parameters with which the experiments were carried out. The process parameters were controlled using manometers with pressure switches available in the plant. In general, the main factors influencing the performance of the thermal arc spraying process are: compressed air pressure, front nozzle geometry, electrical current density, arc-substrate distance, electrical, substrate roughness and wire feed speed.

The thermal arc spraying process followed the technological route presented in the team's previous research [13], accompanied by a number of additional operations specific to the research activity:

- Sampling;
- Preparation of surfaces for metallisation (blasting, threading);
- metallisation (deposition of anchor layer and substrate);
- Macroscopic inspection;
- Preparation of samples for optical and electron microscopy analysis;
- Porosity analysis (sampling, sample preparation, determinations);
- Adhesion analysis of deposited layers (sampling, sample preparation, determinations);
- Assessment of the roughness of the deposited layers (sampling, sample preparation, determinations).

As can be seen, specific studies have been carried out to fully characterise the layers deposited by thermal spraying in an activated electric arc, analysing the chemical, physical and mechanical properties of the deposition and therefore of the layer-support system.

TABLE 3

Technological process parameters

Coating material	Sample preparation	Sample type	$v_{rs}$ [rot/min]	Debit [l/min]	$U_{arc}$ [V]	$v_{dp}$ [m/s]	$v_{as}$ [m/s]	$R_a$ [µm]	$I_{arc}$ [A]	$p_{aer}$ [bar]
75B	sand blasting	round	105	439	30	0.8	36	14.36	250	6.0
75B	sand blasting	flat	—	439	30	0.4	36	14.36	250	6.0

Notations:  $I_{arc}$  – electric current intensity;  $U_{arc}$  – arc voltage;  $v_{rs}$  – rotating speed of the substrate;  $v_{dp}$  – gun moving speed;  $v_{as}$  – wire feed rate;  $R_a$  – substrate roughness;  $p_{aer}$  – compressed air pressure.

## 2.2. Samples characterisation

Several methods were used to analyze the set of samples studied in this paper. The first approach was the morphological characterization, both by direct observation, optical microscopy (Optika SZM Stereomicroscope, Insize Optical Microscope) and scanning electron microscopy (SEM), the Vega Tescan LMH2II electron microscope being used for this purpose, on the High Vacuum module, with a filament voltage of 30 kV. On the SEM is coupled an EDS (Energy-dispersive X-ray spectroscopy) module, that was used for the elemental chemical analysis on various areas of the samples. The samples used for cross-sectional analysis were obtained by embedding a cylindrical section of Cu bar on which the Ni-based coating was deposited in a transparent resin, inside a metal ring with a stiffening role on the outside. The embedded specimens were ground and polished according to metallurgical specimen preparation procedures until a “mirror” polished surface was obtained.

The surface rugosity was studied with the help of Mitutoyo SurfTest 301J Rugozimeter.

### 2.2.1. Coating adherence

The adhesion of nickel-aluminium coatings obtained by thermal arc spraying using 75B wire, diameter  $\varnothing 1.6$  mm as material, can be studied by several methods [14], the one chosen in this study being the tensile test according to SR EN 582/1995 - for flat specimens.

Fig. 1 shows a schematic representation of the device required to clamp the flat specimens in the test machine trays used in this study to determine the deposit adhesion by tensile test. The determinations were carried out on the INSTRON Tensile Compression Tester – Test Class 1 according to EN 10002-2 with constant speed and shock-free loading [15].

In order to determine the tensile bond stress, the value of the force  $F_m$  that causes the layer to peel and the area  $S$  of the fractured area of the metallic layer were determined. The bond stress was calculated using formula (1) according to SR EN 582/1995.

$$R_H = \frac{F_m}{S}, [\text{N}/\text{mm}^2] \quad (1)$$

where:  $F_m$  – maximum load force, [N];  $S$  – the cross-sectional area of the specimen at the breaking face [ $\text{mm}^2$ ].

From Fig. 1 it can be seen that in order to determine the bond strength, an adhesive and a counterpart of the same dimensions as the metallised sample are required. The metallised specimen is bonded to the metallised sample using an adhesive. The adhesive used is POXIPOL, which has a tensile strength of  $\sigma_r = 55.06 \text{ N}/\text{mm}^2$ , provided that the bonded surface has a roughness of  $Ra_{\min} = 12 \mu\text{m}$ .

TABLE 5 shows: the tests used to determine the 75B deposition adhesion, the average thickness of the deposited layer ( $g_{\text{strat}}$ ), the test speed ( $v_{\text{inc}}$ ), the surface area of the layer

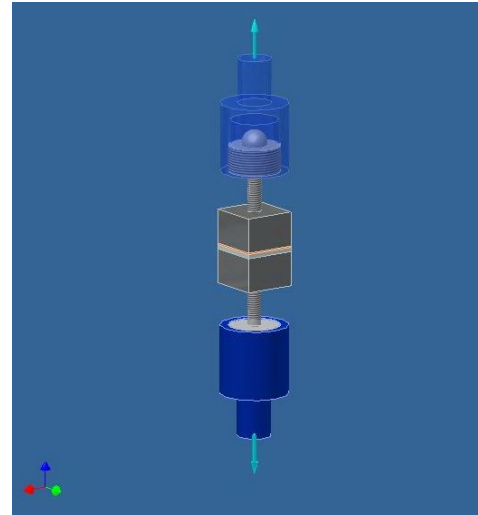


Fig. 1. Device for determining the adhesion of 75B layers by tensile test – according to SR EN582/1995

( $S$ ), the value of the maximum breaking force ( $F_{\text{max}}$ ), the normal stress of the layer ( $R_{Hi}$ ) and the average value of the deposition adhesion ( $\tau_{ad}$  and  $R_H$ ). The value of coating thickness,  $g_{\text{strat}}$  in TABLE 5 was obtained by calculating the arithmetic mean of three measurements taken at different points – according to SR EN ISO 9220/2004.

The tensile strength ( $R_H$ ) was calculated as the average of the maximum stresses recorded on three flat specimens obtained under the same technological conditions – according to SR EN 582/1995. From our own experimental tests we excluded specimens with deposits with surface defects (cracks, fissures) or thicknesses up to 0.5 mm, which were declared “non-compliant” with SR EN 582/1995, i.e. DIN 27201- 0/2005-02.

### 2.2.2. Coating porosity

The porosity of thermally sprayed coatings is expressed by the degree of porosity and is classically determined by standard methods: gravimetric and volumetric. Both methods are based on the infiltration of a liquid (oil, mercury, water) into the coating [16].

In order to determine the degree of porosity of 75B coatings obtained by thermal spraying in an activated electric arc, we used the gravimetric method, which consisted of determining the mass of the deposited coating before and after immersion in oil.

The deposition mass of 75B obtained by thermal spraying in an activated electric arc was determined by weighing the samples before and after metallization, using the formula:

$$G_s = G_{pm} - G_p \quad (2)$$

unde:  $G_s$  – weight of the 75B layer [Kg],  $G_{pm}$  – sample weight after metallisation [Kg],  $G_p$  – initial sample weight [Kg].

Weighing of samples was carried out using the AQT 2600 technical balance for samples where the deposited layer was adherent to the substrate.

The degree of porosity was determined on cylindrical samples ( $\text{Ø}36 \times 40$  mm), with a maximum thickness of the deposited layer of 3 mm. Immersion of the samples was carried out in additivated mineral oil type H46A – STAS 9691/87, obtained from: highly refined base oils, antioxidant additives, corrosion inhibitors, and antifoam.

The gravimetric method for determining the degree of porosity is subjective in that it does not take into account the closed pores in the layer structure. In order to complete the research, we used in parallel, the numerical method (“scanning”) to determine the porosity of the deposit. The method has the advantage that it takes into account the existence of closed pores.

The numerical method for determining the porosity of layers consists of:

- obtaining the color photograph of the microscopic image;
- scanning the image and placing it on the computer’s hard disk;
- selecting a characteristic portion of the deposited layer;
- primary static analysis of the color distribution – which is designed to highlight the frequency of the points that make up the image by color shades;
- selection of the range of characteristic pore colors on the scanned image;
- selection of pores based on the characteristic shade – Fig. 2;
- analysis of the frequency of occurrence of pore-specific colors in the selected image;
- determination of porosity by relating the number of characteristic pore dots to the total number of dots on the image – relation (3).

$$P_n = \frac{N_1}{N} \cdot 100 [\%] \quad (3)$$

where:  $N_1$  = the number of dots representing the pores;  $N$  = the total number of points in the image.

In order to increase the accuracy of the determination it is preferred to convert the scanned image from color shades to black and white shades.

The numerical method requires the use of specialized metallographic image processing software for the percentage determination of pores in the section under analysis. In the research, we used IQ Materials image capture and analysis software (Media Cybernetics – Canada).

The experimentally obtained results (weight of metalized sample –  $G_{pm}$ , weight of immersed sample –  $G_{pi}$ , layer thickness –  $g_{start}$ , deposition density –  $\rho_{dep}$ ) and the working conditions under which the determinations were carried out: oil temperature ( $T_u$ ) = 120°C and immersion time ( $t_i$ ) = 2 hours, are presented in TABLE 4. The gravimetric porosity values –  $P_g$ ,

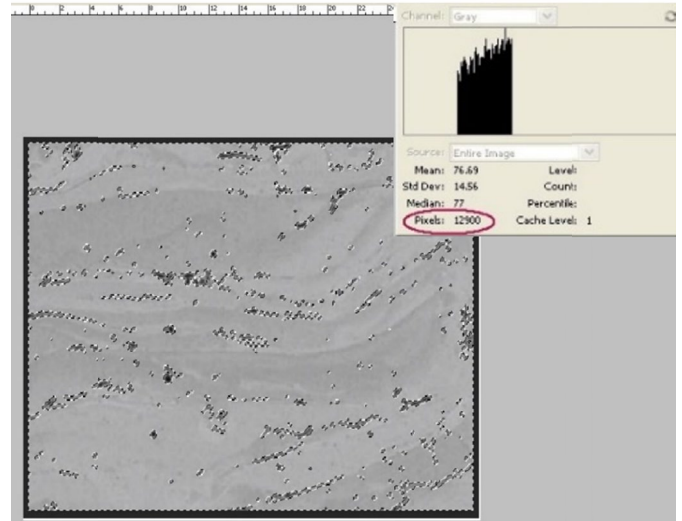


Fig. 2. Total number of pixels representing pores

respectively numerical  $P_n$ , entered in TABLE 4 represent average values obtained from a sample of five determinations carried out on a batch of samples. The determination of the deposition thickness was carried out using the Elcometer 456 and an electron microscope in accordance with SR EN 9920/2006.

### 3. Results and discussions

#### 3.1. Macroscopic aspect, layer roughness and morphology of the 75B thermal arc spraying coatings

The surfaces of the Ni-Al alloy coatings obtained by thermal arc spraying are greyish-grey in color and have a roughness in the range of 8.7-12  $\mu\text{m}$ .

Fig. 3 shows images of the surfaces of the 75B thermal arc-sprayed 75B deposits, both by optical microscopy (OM) on the surface (see Fig. 3a) and in section (Fig. 3b) and by electron microscopy on the surface (Fig. 3c).

The porous structure of the coating surface, typical of such deposits, is observed, which are formed by the continuous overlapping of splats formed by the melt droplets (75B) on impact with the substrate. The detail captured in Fig. 3c) clearly shows such a splat superimposed on the previous layers. In the cross-sectional image (3b)), the top right shows the specific cross-sectional lamellar structure of thermal spray coatings, and the bottom left shows the substrate and the coating-substrate interface.

Regarding the porosity of the coating, from the analysis of the experimentally obtained data, presented in TABLE 4, the

TABLE 4

Experimental results at porosity determination

$T_u$ [°C]	$t_i$ [h]	$g_{strat}$ [mm]	$G_{pm}$ [kg]	$G_{pi}$ [kg]	$\rho_{dep}$ [kg/dm <sup>3</sup> ]	Average porosity		
						$P_g$ [%]	$P_n$ [%]	$\Delta P$ [%]
120	2	2.57	0.33107	0.38176	6.18	15.31	16.99	1.68

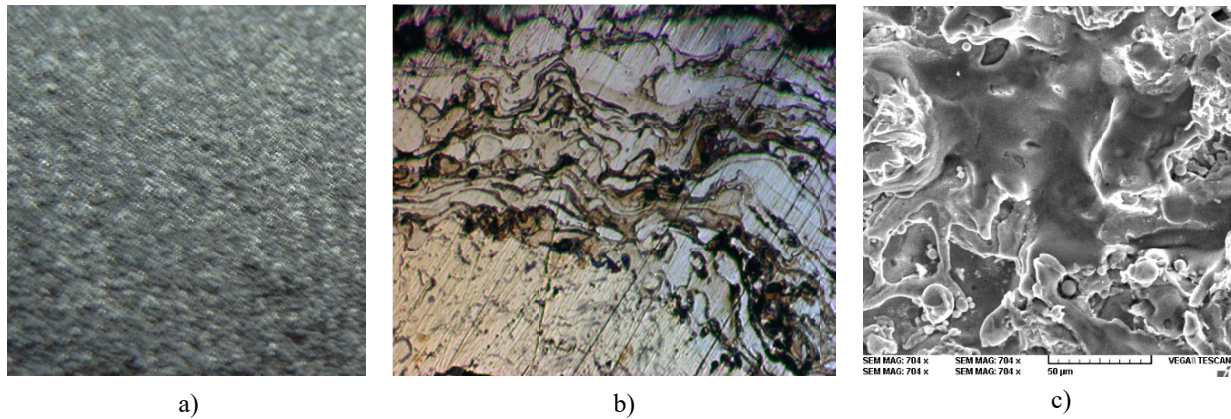


Fig. 3. Representative images of coating 75B: a) photograph of coating surface (60×), b) OM image of coating cross-section (200×), c) SEM image of coating surface (700×)

following aspects can be observed: the resulting coating has a uniform appearance, has good adhesion to the substrate surface, and the porosity is within acceptable limits.

### 3.2. Investigations on the chemical composition of 75B deposits deposited by thermal arc spraying

Mappings of the main alloying chemical elements in the substrate (Cu-based alloy) – deposition (75B) assembly on cylindrical specimens (see Fig. 4) are shown in Fig. 5. Fig. 6 shows the distribution of the main alloying elements at the layer-substrate interface on the cross-section of the specimen. Indicatively, the

average chemical composition existing over the area shown in Fig. 6 is given in TABLE 2.

Fig. 6a) shows the distribution of chemical elements in the cross-section of a system (CW024A) – layer (75B), obtained at high values of electric current intensity. The corresponding chemical element spectrum is shown in Fig. 6b).

The variation of the concentration of the main alloying elements following a direction perpendicular to the layer-substrate interface is shown in Fig. 7. It can be noticed, from the presented figures, the presence of Cu inside the Ni layer.

Morphological analysis of Ni layers obtained by thermal arc spraying shows that they exhibit homogeneity of chemical composition.

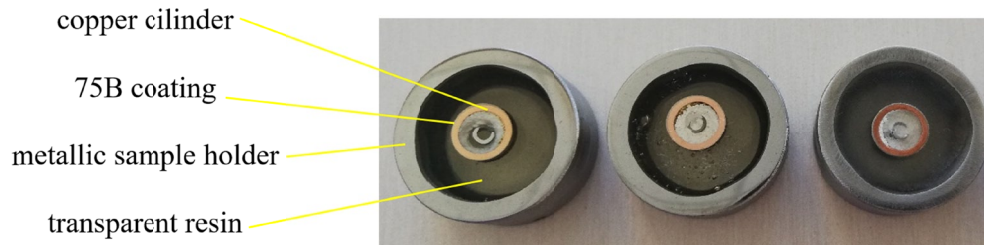


Fig. 4. Specimens on which chemical element analysis was performed

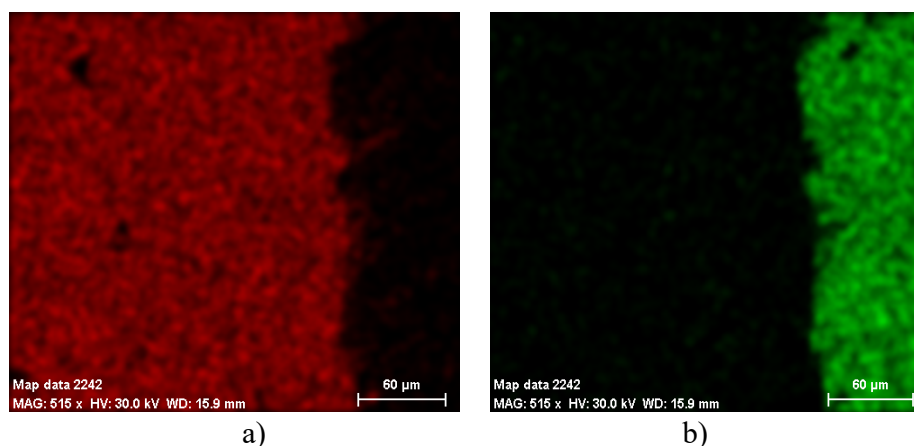


Fig. 5. Mapping of the main alloying elements in the substrate (CW024A) – layer (75B) system: a) Cu distribution in substrate (500×); b) Ni distribution in layer (500×)

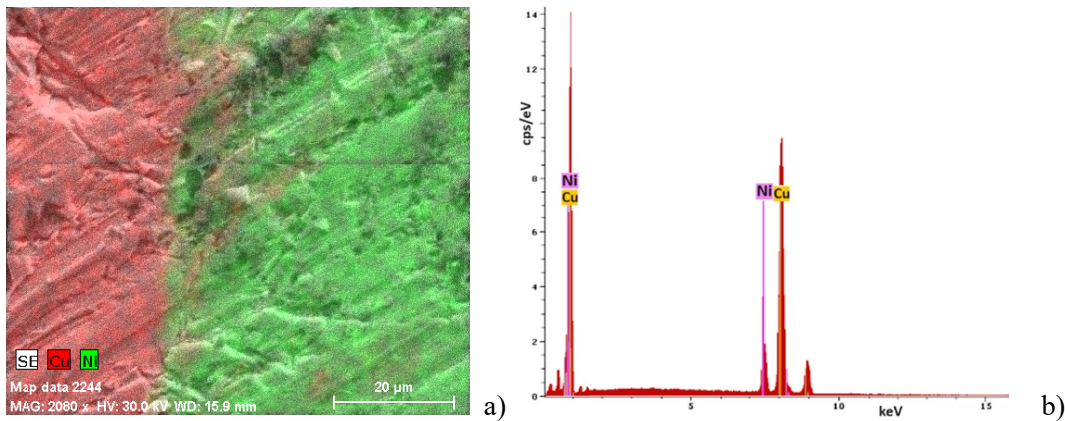


Fig. 6. a) Distribution of main chemical elements in the cross-section of a system (CW024A) – layer (75B), b) Spectrum of chemical elements on the scanned surface

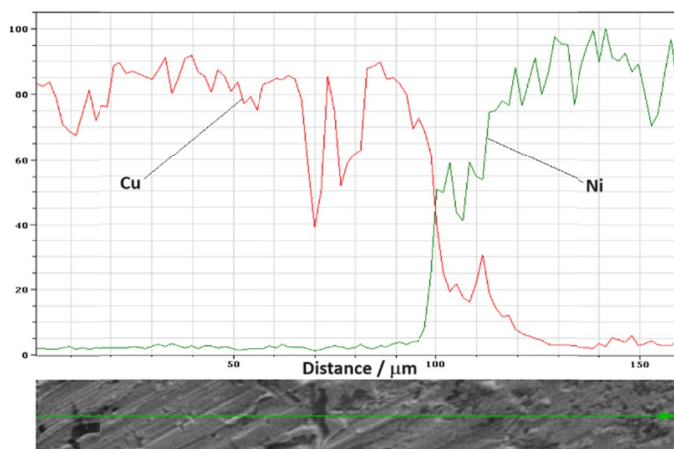


Fig. 7. Distribution of the main alloying elements along a perpendicular direction on the layer-substrate interface

The absence of aluminum in the layer is noted, although it is an alloying element of the additive material (75B wire) in the case of deposition obtained at high values of electric current intensity. This can be explained by the fact that the high deposition temperature (obtained by increasing the electric current intensity) causes the evaporation of aluminum from the deposition material (wire 75B) – see Figs. 5, 6 and TABLE 1.

At high values of the electric current intensity, as well as at high sputtering pressures, the presence of Cu inside the Ni layer is noticeable – see Figs. 6 and 7. This can be explained by the fact that the glowing Ni particles, when hitting the substrate surface, cause the melting of the Cu asperities and thus the formation of a transition zone formed by a Cu-Ni pseudo-alloy.

### 3.3. Determination of adhesion of Ni-Al coatings obtained by thermal arc spraying

As can be seen from the data presented in TABLE 5, the  $R_{Hi}$  adhesion values as well as the average  $R_H$  adhesion value is close to the value of  $R_H = 13.11 \text{ N/mm}^2$  – the average technical characteristic guaranteed by the manufacturer, for the 75B coating material.

Fig. 8 shows the fracture surfaces resulting from the determination of deposition adhesion by tensile test. The images show that the breakage occurred at the interface of the adhesive substrate or adhesive layer, which shows that the breakage was good.

It can be seen that the average adhesion of the deposits obtained is acceptable, being close to the adhesion value of 75B deposits guaranteed by the manufacturer in the product data sheet for this material quality ( $16.5 \text{ N/mm}^2$ ).

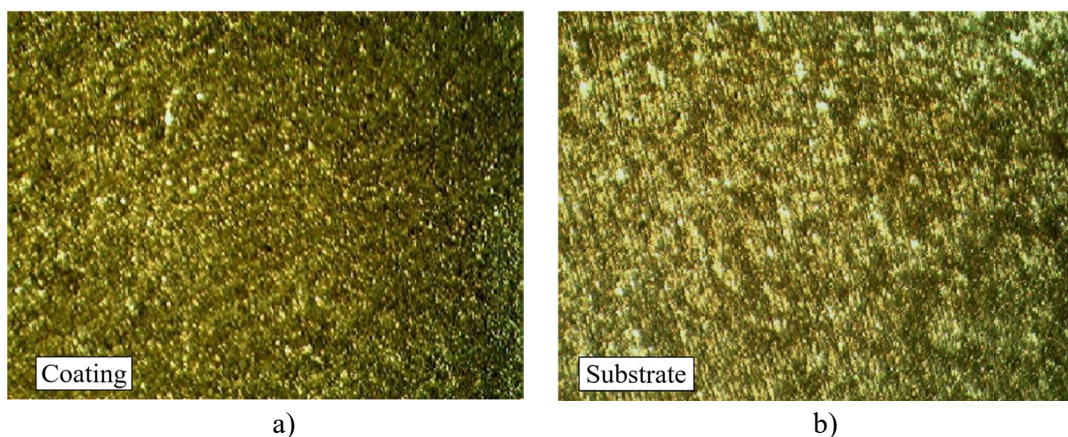


Fig. 8. Stereomicroscope images of adhesive-breakage surfaces (10×): a) adhesive-layer interface; b) adhesive-substrate interface

Values obtained during the tests

$v_{inc}$ [N/s]	$g_{strat}$ [mm]	$S$ [mm <sup>2</sup> ]	$F_{max}$ [N]	$R_{HI}$ [N/mm <sup>2</sup> ]	Average adherence
					$R_H$ [N/mm <sup>2</sup> ]
10	2.61	802.12	11630.92	14.05	13.24

#### 4. Conclusions

Morphological analysis of Ni layers obtained by thermal arc spraying shows that they exhibit homogeneity of chemical composition.

The absence of aluminum in the layer is noted, although it is an alloying element of the additive material (75B wire) in the case of deposition obtained at high values of electric current intensity. This can be explained by the fact that the high deposition temperature (obtained by increasing the electric current intensity) causes the evaporation of aluminum from the filler material (wire 75B).

Since a high value of the electric current intensity as well as the sputtering pressure was chosen, the presence of Cu inside the Ni layer is noticed. This can be explained by the fact that the glowing Ni particles, when hitting the substrate surface, cause the melting of Cu asperities and thus the formation of a transition zone composed of a Cu-Ni pseudo-alloy.

The average adhesion of the deposits obtained is acceptable, being close to the 75B deposit adhesion value guaranteed by the manufacturer in the product data sheet for this material grade (16.5 N/mm<sup>2</sup>).

The experimental investigations carried out on the properties of nickel-aluminium (75B) deposits obtained by thermal arc spraying, combined with the existing data in the technical literature, validated the theoretical model accepted for analysis.

#### REFERENCES

- [1] J.R. Davis ed., ASM Specialty Handbook: Copper and Copper Alloys. ASM International 652 (2001). ISBN 0-87170-726-8.
- [2] V. Protsenko, T. Butyrina, D. Makhota, S. Korniy, F. Danilov, Modification of Surface Morphology and Surface Properties of Copper-Nickel Alloy by Anodic Treatment in a Deep Eutectic Solvent (Ethaline). Arch. Metall. Mater. **68** 2, 477-482 (2023). DOI: <https://doi.org/10.24425/amm.2023.142425>
- [3] J. Aroma, M. Kekkonen, M. Mousapour, A. Jokilaakso, M. Lundström, The Oxidation of Copper in Air at Temperatures up to 100°C. Corros. Mater. Degrad. **2** (4), 625-640 (2021). DOI: <http://dx.doi.org/10.3390/cmd2040033>
- [4] J.R. Davis (Ed.), Handbook of thermal spray technology, ASM International, Materials Park, OH, USA, 2004.
- [5] Y.-J. Hwang, K.-S. Kim, J.-S. Park, K.-A. Lee, Manufacture of MoO<sub>3</sub> Coating Layer Using Thermal Spray Process and Analysis of Microstructure and Properties. Arch. Metall. Mater. **67** 4, 1535-1538 (2022). DOI: <https://doi.org/10.24425/amm.2022.141089>
- [6] L. Pawlowski (Ed.), The Science and Engineering of Thermal Spray Coatings, (1995) John Wiley & Sons Ltd, New York.
- [7] S.L. Toma et al., Hard Alloys with High Content of WC and TiC – Deposited by Arc Spraying Process. In: Welding – Modern Topics, S.C.A. Alfaro, W. Borek, B. Tomiczek (eds.), IntechOpen, London (2020). DOI: <https://doi.org/10.5772/intechopen.94605>
- [8] V. Goanta, C. Munteanu, S. Müftü, B. Istrate, P. Schwartz, S. Boese, G. Ferguson, C.I. Moraras, Evaluation of the Fatigue Behaviour and Failure Mechanisms of 52100 Steel Coated with WIP-C1 (Ni/CrC) by Cold Spray. Materials **3609**, 15 (2022). DOI: <https://doi.org/10.3390/ma15103609>
- [9] S. Lupescu, C. Munteanu, A. Tufescu, B. Istrate, N. Basescu, Contact stress simulation problem in case of the Mg alloys, IOP Conference Series: Materials Science and Engineering **997**, 1 (2020). Article number 012024. DOI: <https://doi.org/10.1088/1757-899X/997/1/012024>
- [10] C.C. Paleu, C. Munteanu, B. Istrate, S. Bhaumik, P. Vizureanu, M.S. Bălțatu, V. Paleu, Microstructural Analysis and Tribological Behavior of AMDRY 1371 (Mo–NiCrFeBSiC) Atmospheric Plasma Spray Deposited Thin Coatings. Coatings **10** (12), 1186 (2020). DOI: <https://doi.org/10.3390/coatings10121186>
- [11] C. Paulin, D.L. Chicet, B. Istrate, M. Panturu, C. Munteanu, Corrosion behavior aspects of Ni-base self-fluxing coatings. IOP Conference Series: Materials Science and Engineering **147**, 012034 (2016). DOI: <https://doi.org/10.1088/1757-899X/147/1/012034>
- [12] W. Tillmann, L. Hagen, D. Stangier, I.-A. Laemmerhirt, D. Biermann, P. Kersting, E. Krebs, Wear behavior of bio-inspired and technologically structured HVOF sprayed NiCrBSiFe coatings. Surf. & Coatings Technology **280**, 16-26 (2015). DOI: <https://doi.org/10.1016/j.surfcoat.2015.08.055>
- [13] S.L. Toma, D.-L. Chicet, A.-M. Cazac, Numerical Calculation of the Arc-Sprayed Particles' Temperature in Transient Thermal Field. Coatings **12**, 877 (2022). DOI: <https://doi.org/10.3390/coatings12070877>
- [14] A.S. Maxwell, Review of test methods for coating adhesion, 2001, NPL Report MATC (A) 49, National Physical Laboratory, Teddington, Middlesex, UK, ISSN 1473-2734.
- [15] M.A. Calin, A. Curteza, St. Toma, M. Agop, Morphological properties of polyamide 6-cnt nanofibers obtained by electrospinning method. Revista Metalurgia International **18**, 19-22 (2013). ISSN 1582-2214.
- [16] A.M. Cazac, C. Bejinariu, C. Baciuc, S.L. Toma, C.D. Florea, Experimental Determination of Force and Deformation Stress in Nanostructuring Aluminium by Multiaxial Forging Method. Applied Mechanics and Materials **657**, 137-141 (2014). DOI: <https://doi.org/10.4028/www.scientific.net/AMM.657.137>